GEOPHYSICS, VOL. 66, NO. 6 (NOVEMBER-DECEMBER 2001); P. 1947–1959, 10 FIGS.

Seismic sequence analysis and attribute extraction using quadratic time-frequency representations

Philippe Steeghs* and Guy Drijkoningen‡

ABSTRACT

The variation of frequency content of a seismic trace with time carries information about the properties of the subsurface reflectivity sequence. As a result, analysis of the data in terms of the local frequency content can provide a worthwhile addition to the standard procedures that are used in seismo-stratigraphic interpretation. The theory of quadratic time-frequency representations provides a solid foundation for local frequency analysis of seismic data and seismic attribute extraction. Two applications of the quadratic time-frequency representations are demonstrated: seismic sequence analysis and seismic attribute extraction. The joint time-frequency representation of a seismic reflection pattern is often much more easily interpreted in terms of subsurface stratification than the time-or frequency-domain description alone. We show how the time-frequency representation can be used to delineate seismic sequences on the basis of the time-frequency characteristics of the signal. There exists a close relation between complex-trace attribute analysis and quadratic time-frequency representations. In the time-frequency approach, the seismic attributes are characteristics of the local spectrum. Extraction of the attributes from the time-frequency representation of the seismic trace leads to considerable improvement of the signal-to-noise ratio of the attributes. Furthermore, the classic set of seismic attributes of instantaneous amplitude, phase, and frequency can be easily extended with other parameters describing the local spectrum, such as instantaneous bandwidth, skewness, and kurtosis.

INTRODUCTION

The frequency content of a seismic trace is primarily determined by the bandwidth of the outgoing seismic pulse and the absorption characteristics of the subsurface. However, the variations within this band are primarily the result of changes in the timing of seismic events. These changes may result from thickness variations or a strong lateral change in interval velocity. Assuming that the seismic section represents the band-limited reflectivity of the subsurface, the variations in spectral content of the seismic trace can be used to characterize the stochastic properties of the reflectivity. The power spectrum, which shows how the energy of a signal is distributed over frequency, is the most commonly used representation to analyze the spectral content of a data sequence. However, the power spectrum does not reveal whether the frequency content changes with time and where these changes occur. Hence, for studying variations in spectral content, we need an extension of the global power spectrum to a representation that localizes the energy of the signal both in time and in frequency. There are many ways to devise such a joint time-frequency representation, and it largely depends on the type of signal under analysis which one performs best in terms of resolution and readability. In this paper, we discuss the class of quadratic time-frequency representations of which the Wigner distribution and the spectrogram are the most widely known (Hlawatsch and Boudreaux-Bartels, 1992; Cohen, 1995). This class of representations provides a natural framework for complex-trace attribute analysis. The instantaneous frequency, for instance, can be considered as the mean frequency as a function of time of a joint time-frequency representation. The relation between time-frequency representations and seismic attributes has been discussed by Barnes (1993a) and Bodine (1986). This paper provides a more general framework that also incorporates their approach. We will exploit the relation between the complex-trace description and the time-frequency representation to clarify some of the properties of complex-trace attributes and to develop more robust methods for seismic attribute extraction. Furthermore, using the time-frequency approach, we can also define new attributes, such as instantaneous bandwidth and third- and fourth-order statistical measures.

Manuscript received by the Editor November 6, 1998; revised manuscript received March 13, 2001.
*Formerly Rice Consortium for Computational Seismic Interpretation, Department of Electrical and Computer Engineering, Rice University, Houston, Texas 77005-1892; presently TNO Physics and Electronics Laboratory, Post Office Box 96864, 2509 JG, The Hague, Netherlands. E-mail: steeghs@fel.tno.nl.
‡Delft University of Technology, Department of Civil Engineering and Geosciences, P.O. Box 5028, 2600 GA, Delft, The Netherlands. E-mail: g.g.drijkoningen@ta.tudelft.nl.

The paper is organised as follows. We first introduce the time-frequency representations of the quadratic class. The mathematical properties of these time-frequency representations and their relation to complex-trace attribute analysis are discussed in an Appendix. We discuss two applications of the method in more detail: seismic sequence analysis and attribute extraction.

TIME-FREQUENCY REPRESENTATIONS

The most straightforward approach to obtain a time-frequency representation is to divide the signal into short time segments and determine the spectrum of each segment by means of a Fourier transformation. The result of this operation is the short-time or sliding-window Fourier transform. If we weight the data at each time t with a window function $w(t)$, a modified signal $u_t(\tau)$ is obtained as

$$u_t(\tau) = u(\tau)w(t-\tau). \tag{1}$$

The sliding window Fourier transform, $\hat{u}_t(f)$, is given by

$$\hat{u}_t(f) = \int_{\tau\in\mathbb{R}} \exp(-\mathrm{j}2\pi f\tau)u_t(\tau)\,d\tau. \tag{2}$$

Repeating this procedure for each time t and taking the squared modulus of $\hat{u}_t(f)$, we obtain the time-frequency representation

$$S(t;f) = |\hat{u}_t(f)|^2, \tag{3}$$

which is the *spectrogram* of the signal. A problem associated with the spectrogram is that the result is strongly influenced by the choice of window function $w(t)$. The windowed signal $u_t(\tau)$ and the local spectrum are a Fourier transform pair. Consequently their broadness in time and frequency is governed by the uncertainty principle. Improving time localization by using a shorter window, results in a broadening of the local spectrum and, consequently, frequency localization deteriorates. The reverse happens when lengthening the time window. In that case, frequency localization is improved at the cost of time localization. Figure 1 illustrates this property of the spectrogram. A seismic trace is analyzed with both a short-time window (Figure 1b) and a long window (Figure 1c). The localization of energy in the joint time-frequency domain is strongly dependent on the duration of the analysis window. In the short-window spectrogram, we observe that the signal components are well localized in time, but we have poor frequency localization. If we increase the window size, frequency localization is improved, but time localization deteriorates.

Improvement of the resolution of the sliding-window Fourier transform was one of the motivations behind the development of other techniques for the analysis of nonstationary signals. An effective way to minimize window effects is use an analysis window that is matched to the signal. For certain types of signals, excellent results can be achieved by using the reverse of the signal as an analysis window. Using the reversed signal as a window function, we obtain the time-frequency representation,

$$W(t;f) = \int_{\tau\in\mathbb{R}} \exp(-\mathrm{j}2\pi f\tau)u\left(t+\frac{1}{2}\tau\right)u^*\left(t-\frac{1}{2}\tau\right)d\tau, \tag{4}$$

where the asterisk denotes complex conjugation. The time-frequency representation $W(t;f)$ is the Wigner distribution of $u(t)$ (Claasen and Mecklenbräuker, 1980). Because the signal now enters twice into the representation, the representation is called a quadratic or bilinear time-frequency representation. In Appendix A, we discuss some of the mathematical properties of the Wigner distribution.

Figure 1d shows the Wigner distribution of the seismic trace. The localization of energy in the time-frequency plane has considerably improved. However, a striking feature of the Wigner distribution is the oscillating ridges between two signal components at (t, f)-locations where no energy is expected. These cross terms are an expression of the quadratic nature of the Wigner distribution. The interference of these cross terms complicates the interpretation of the Wigner distribution of most real-world signals. However, for many signals, these cross terms can be suppressed by smoothing the Wigner distribution over time and frequency, i.e.,

$$P(t;f) = \int_{t'\in\mathbb{R}}\int_{f'\in\mathbb{R}} \Psi(t';f')W(t-t';f-f')\,dt'\,df'. \tag{5}$$

The smoothing function $\Psi(t;f)$ is called the *kernel* of the time-frequency representation. Each particular kernel results in a different time-frequency representation, and the properties of this time-frequency representation can be derived from the properties of the associated kernel (Appendix A). The

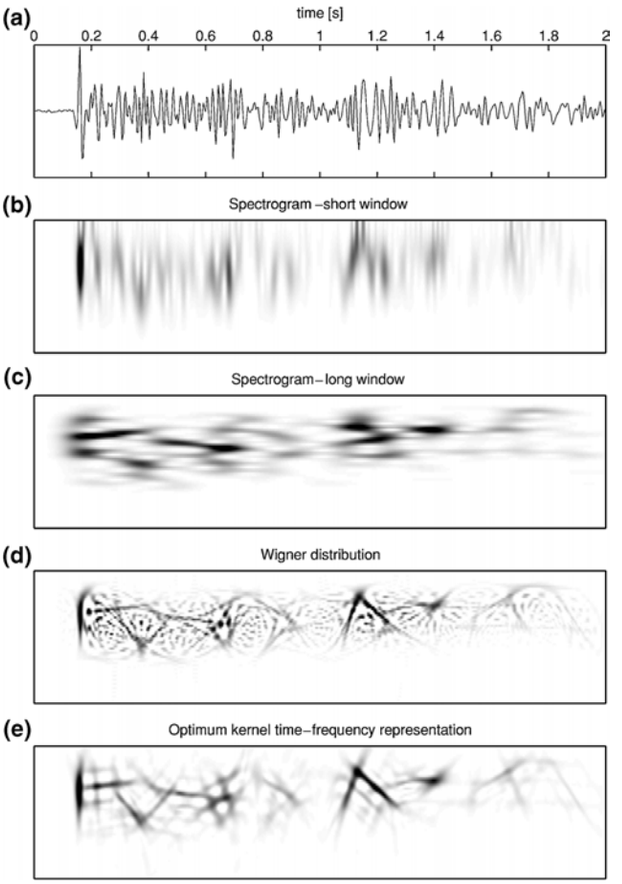

FIG. 1. (a) A seismic trace and (b) Spectrogram using a long window, (c) short-window spectrogram, (d) Wigner distribution, and (e) adaptive optimum kernel time-frequency represention. Horizontal axis is time, vertical axis is frequency.

class of time-frequency representations that can be obtained by smoothing the Wigner distribution is called Cohen's class (Cohen, 1989, 1995). The spectrogram of equation (3) is also a member of this class. For the spectrogram, the associated smoothing kernel is the Wigner distribution of the analysis window $w(t)$. In the Fourier domain, the two-dimensional convolution of equation (5) transforms into a two-dimensional filter operation. The design of these filters, one tries to maximize the suppression of the cross terms while compromising other desirable properties of the time-frequency representation as little as possible. For instance, there is a trade-off between preservation of the resolution (minimal smoothing) and the degree of cross-term suppression (maximal smoothing). The location and amplitude of the cross term depends on the signal. Consequently, this trade-off can be optimized by adapting the shape of the smoothing kernel to the characteristics of the signal under analysis. Optimum kernel design for quadratic time-frequency representations is discussed in Appendix A. An adaptive optimum kernel time-frequency representation of the seismic trace is shown in Figure 1e. The cross terms have been largely suppressed, while at the same time the resolution has not deteriotated much compared to the Wigner distribution. Note that both short-duration signal components (pulses) and long-duration components (tones) are localized equally well. It is this ability to sharply localize energy in both time and frequency that makes the optimum kernel time-frequency representation very well suited for local spectral analysis of seismic signals.

SEISMIC SEQUENCE ANALYSIS

In order to relate the parameters that can be extracted by signal analysis to a subsurface model, some assumptions and simplifications have to be made with regard to the physics involved in a seismic experiment. The first corollary is related to the physical model that links the seismic sequence to stratification. It is assumed that the seismic reflection data represent a band-limited reflection coefficient sequence. This is a strong assumption, because we know that seismic data we measure at the surface is generally quite remote from a primary-only, acoustic, reflection response. Many other wave phenomena are present in our data, such as multiple reflections, energy conversions from longitudinal to shear waves, and anelastic effects giving rise to attenuation and dispersion. The goal of seismic preprocessing and migration is to remove all wave phenomena, other than the specular reflections from impedance contrasts. Hence, the assumption can be phrased differently by saying that it is assumed that the seismic processing did its work and the time-frequency representation of our data is a good approximation of the time-frequency representation of the subsurface reflection response within the source bandwidth. As there is a one-to-one time-depth relation between the time and depth reflectivity functions, we assume that an event that is localized in time in the time-frequency representation of the data is an expression of the stratification of impedance at the corresponding depth.

The second corollary pertains to the method that is used for modeling of the seismic response. The synthetic examples in the section were generated using a plane-wave modeling scheme based on the reflectivity method (Fuchs and Müller, 1971; Fokkema and Ziolkowski, 1987). The input model is that of a layered earth, where the layers are bounded by impedance discontinuities. Gradual changes in impedance are therefore approximated by replacing them by thin layers with small reflection coefficients between them. Although this is not a trivial step, it will be shown that in the cases presented here, the assumption of a layered earth leads to synthetic seismic data that can closely match the measured data. The examples all represent the vertical incidence response, which precludes the presence of angle-dependent effects and longitudinal-to–shear-wave energy conversion. However, internal multiple reflections have been included in the modeling.

Our model of a seismic sequence is based on the observation that a seismic reflection profile on the scale of several hundreds of meters consists of a limited number of strong reflections. Between these major boundaries, one usually observes a seismic reflection pattern that results from closely spaced impedance contrasts that cannot be resolved individually. The strong reflections are usually associated with sequence boundaries, and the interference composites determine the seismic facies. An idealized depth model of this type of impedance distribution is shown in Figure 2, together with its seismic reflection response. The model is that of a layered sequence between two homogeneous layers. The mean velocity of the sequence is 2000 m/s. The velocity fluctuation consists of two types of components. The first type of component is a harmonic variation. There are two components of this type in the model. They both have an amplitude of 50 m/s and spatial frequencies of, respectively, 0.1 and 0.125 1/m. The second component has an amplitude of 50 m/s and a spatial frequency that increases with depth at a rate of 0.0003 m^{-2}. In the depth model, the density has been kept constant at 1000 kg/m^3. Note that it is not possible to distinguish the individual components in the time response.

In Figure 3 we show time-frequency representation of the synthetic seismic trace. The spectrum of the seismic response shows two peaks at frequencies 100 and 125 1/s, related to the

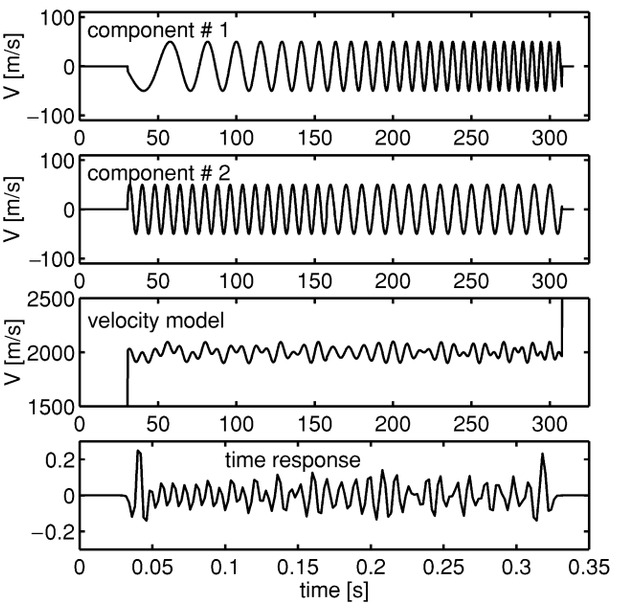

FIG. 2. Components of the velocity model, velocity depth model, and seismic response to the depth model.

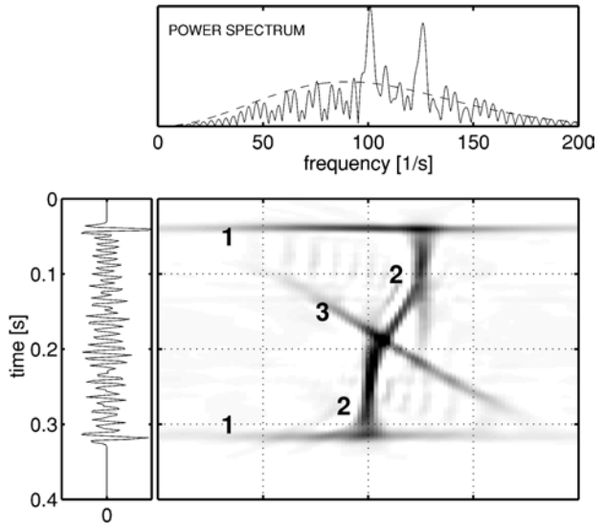

FIG. 3. Time-frequency representation of the seismic response to the depth model.

harmonic components of the stratification. Apart from these two peaks, the shape of the amplitude spectrum of the seismic reflection response follows that of the source pulse (dashed line). The three components of the stratification and the boundaries of the sequence show up as separate entities in the time-frequency plane. The strong reflections from the top and base of the sequence are visible as two impulse type components (denoted by a 1 in the figure). The energy that is reflected on two harmonic components (2) is located on a ridge at frequencies 100 and 125 1/s. The linear increase of frequency with depth of component (3) results from the increase of spatial frequency with depth of the third component of the velocity fluctuation.

In Figure 4, we show some seismic modeling results for four one-dimensional seismic sequences. The response to the reflectivity was modeled in the frequency domain and then band limited with a 70 1/s Ricker wavelet. Internal multiples were taken into account in the modeling. Each of the models has a first layer with a thickness of 200 m on top. Velocity and density in the first layer of the model are 1500 m/s and 1000 kg/m^3, respectively.

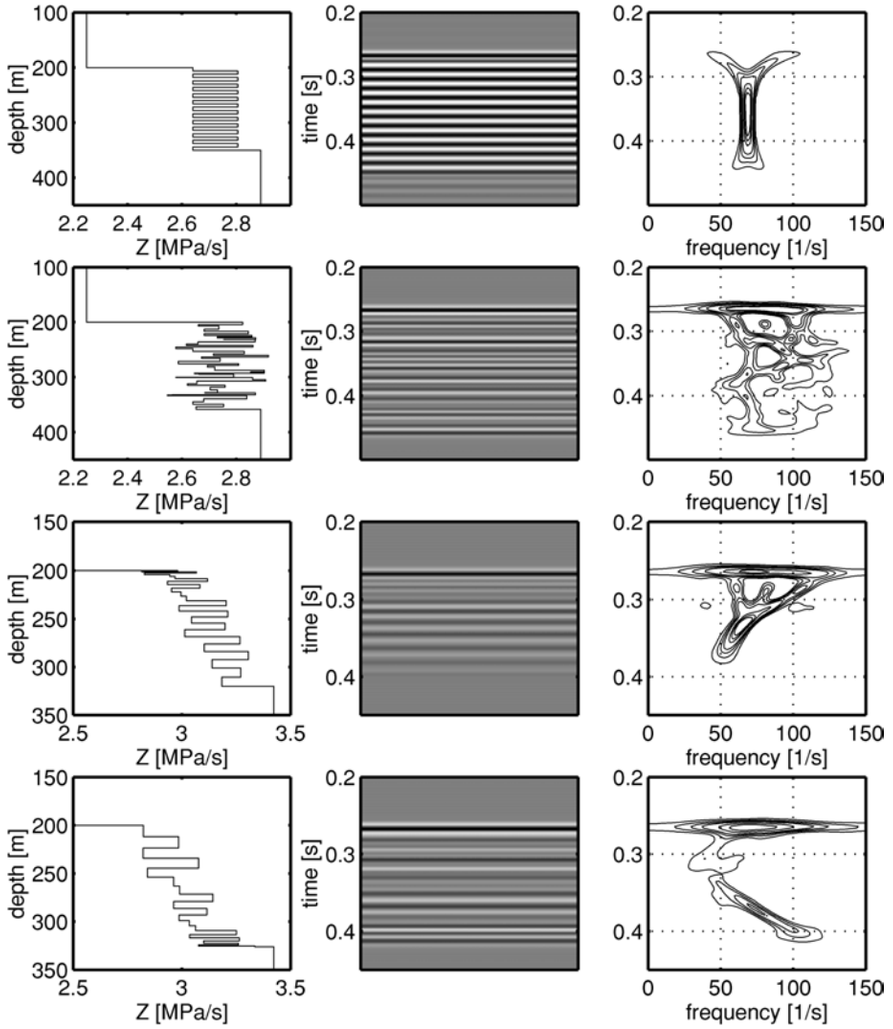

FIG. 4. One-dimensional impedance depth models, seismic response, and time-frequency representation of the synthetic seismic trace.

The first sequence has layers of constant thickness of 6 m. The velocity of the layers alternates between 1625 and 1675 m/s. This type of sequence is also known as a binary sequence. A set of two layers is called a motif. The band width of the reflected signal from this type of sequence is narrow around the frequency of the response to one motif and integer multiples of this frequency. In this case, the temporal frequency of one motif is around 69 1/s. Higher frequency bands are not observed because they are outside the frequency band of the source pulse. Although this is not immediately apparent in the time-frequency representation shown here, the transfer of energy from primary to multiple reflections results in an attenuation of the primary pulse and delay of the arrival of energy. An elaborate discussion of the seismic response to this type of sequence can be found in Morlet et al. (1982).

The second sequence consists of 50 layers with randomly distributed thicknesses and velocities. The mean thickness is 3 m and the maximum deviation of the (uniform) random component of the thickness is 2 m. The velocity is 1650 m/s with a maximum deviation of 130 m/s. Density was taken proportionally to the velocity. The random thicknesses and velocities result in a time-frequency representation of the reflection pattern with no evident relation between time and frequency localization of the energy.

The third and fourth sequences are a combination of Gaussian-distributed alternating velocities, superposed on a linear velocity gradient. Their main feature is an increase of layer thickness with depth for the third sequence and a decrease of layer thickness with depth for the fourth sequence. Both models consist of 25 layers with thicknesses ranging between 0.5 and 12 m. In sequence 3, the thickness of the layers increases with depth, and this model may serve as a model for a depositional sequence in which the rate of sedimentation decreases with geologic time. The thickness of layers in the fourth sequence decreases with depth, which would happen if sediment input increases as a function of geologic time.

The change of layer thickness gives rise to frequency tuning of the response towards the frequency of the (time) thickness of the layering. As a result, these gradual changes in layer thicknesses can be recognized in the time-frequency representation of the seismic signal as a change of frequency content as a function of seismic traveltime. These synthetic data examples demonstrate that the contribution of the stratification of the impedance to the frequency content of a reflected signal is elicited by the time-frequency representation of the data. The time-frequency representation effectively maps the reflection response into an time-frequency pattern from which the reflection configuration can be interpreted more easily than from the time image.

Figure 5 illustrates the application of time-frequency sequence analysis to field data. The seismic section is a part of a regional 2-D seismic line from the Alboran Sea. A standard seismic processing sequence was applied to the data, followed by f-k migration. In the time-frequency representations of the first and last trace of the section, we can distinguish three components in the upper part (0–0.5 s) in both time-frequency representations. The resemblance of the upper part of the two time-frequency representations indicates that the properties of the signal remain fairly constant over a large spatial range. In a seismic facies interpretation, we can describe this part of the section as consisting of continuous events with little change of reflector spacing as a function of lateral distance. The first component is the reflection from the high contrast at the sea bottom, which shows up as an impulselike event in the time-frequency plane. Below the sea-bottom reflector, we observe an increase of frequency with time until approximately $t = 0.35$ s. At $t = 0.35$ s, there is an abrupt change, and a decrease of frequency time occurs until 0.5 s. Below 0.5 s, the energy is less well localized in the time-frequency representations, indicating a more randomly stratified subsurface. The localization of energy in the lower part of the first trace is clearly different than in the last trace. This difference can be attributed to a change of bed spacing with offset. Hence, an evaluation of time-frequency representation results in a division of the seismic section into two seismic units. In the upper unit (0–0.5 s), we can distinguish three separate components, of which one is the sea bottom reflection. The other two time-frequency components enable a further subdivision of the upper unit into two subunits.

Although the time-frequency representation itself provides a clear display of seismic facies characteristics, it will be difficult to use in a routine seismic facies analysis. Computing the time-frequency representation for each trace in a seismic section results in a three-dimensional data volume. The size of this data volume will clearly complicate the interpretation of the time-frequency representation. However, we can attempt to reduce the amount of data by describing the time-frequency representation with a limited number of parameters. For example, we separate the time-frequency representation $P(t; f)$ into two time-frequency representations: one that only has components with an increasing frequency as a function of time, $U(t; f)$, and another that only has components that show a decrease of frequency as a function of time, $D(t; f)$. We can separate these components in the two-dimensional Fourier transform of the time-frequency representation because each type occupies a different half-plane in the transformed domain. We map the result onto a one-dimensional parameter,

$$g(t) = \frac{\int |U(t; f)| - |D(t; f)|\, df}{\int |P(t; f)|\, df}. \qquad (6)$$

The parameter $g(t)$ measures the relative contribution of each type of component to the total energy of the signal as a function of time. The result is plotted in Figure 5c. Darker shades indicate that more energy is found in components that have an increasing frequency as a function of traveltime. We can now clearly distinguish the two units. The upper unit shows little spatial variation, and the three subunits can be clearly distinguished. The frequency remains fairly constant in the first 0.15 s, there is an overall increase in frequency between 0.15 and 0.35 s and decrease between 0.35 and 0.5 s. The lower unit shows large variation as a function of offset and time, indicating a less pronounced stratification pattern. Jurado and Comas (1992) consider the seismo-stratigraphic interpretation of seismic reflection data from the same region. The part of the section shown here coincides with their facies unit I, consisting of sediments of Pliocene to recent age. They divide the unit into two subunits that are separated by an unconformity. The result of the time-frequency analysis confirms this division and adds a further refinement by the subdivision of the upper unit.

SEISMIC ATTRIBUTE EXTRACTION

The complex-trace attributes, first introduced to seismic interpretation by Taner and Sheriff in 1977, are still widely used for the characterization of waveforms. The complex-trace description and the general class of quadratic time-frequency representations are intimately related (Appendix A). In the complex-trace notation, the seismic trace is an analytic signal given by

$$u^a(t) = a(t)\exp(\mathrm{j}2\pi\phi(t)), \tag{7}$$

where $a(t)$ is the instantaneous amplitude and $\phi(t)$ is the instantaneous phase. The complex-trace instantaneous frequency $f^c(t)$ is the derivative of the instantaneous phase,

$$f^c(t) = \frac{1}{2\pi}\frac{d\phi(t)}{dt}. \tag{8}$$

The instantaneous frequency can be estimated directly using a discretized version of equation (8). Unfortunately, such an estimate is highly susceptible to noise. However, the instantaneous frequency can also be estimated from the time-frequency representation. The mean frequency of the time-frequency representation as a function of time, $f^m(t)$, is given by

$$f^m(t) = \frac{\int f P(t; f)\, df}{E(t)}, \tag{9}$$

where $E(t)$ is the time marginal $E(t) = \int P(t; f)\, df$. Hence, the mean frequency is the first moment of the time-frequency representation, normalized by the energy. For the Wigner distribution, the complex-trace instantaneous frequency and $f^m(t)$ are equivalent [equations (A-8)–(A-14)]. However, for a smoothed Wigner distribution, the relation between $f^m(t)$ and $f^c(t)$ is determined by the properties of the smoothing kernel. If the constraints on the kernel given in equations (A-24) and (A-25) hold, $f^c(t)$ and the average frequency

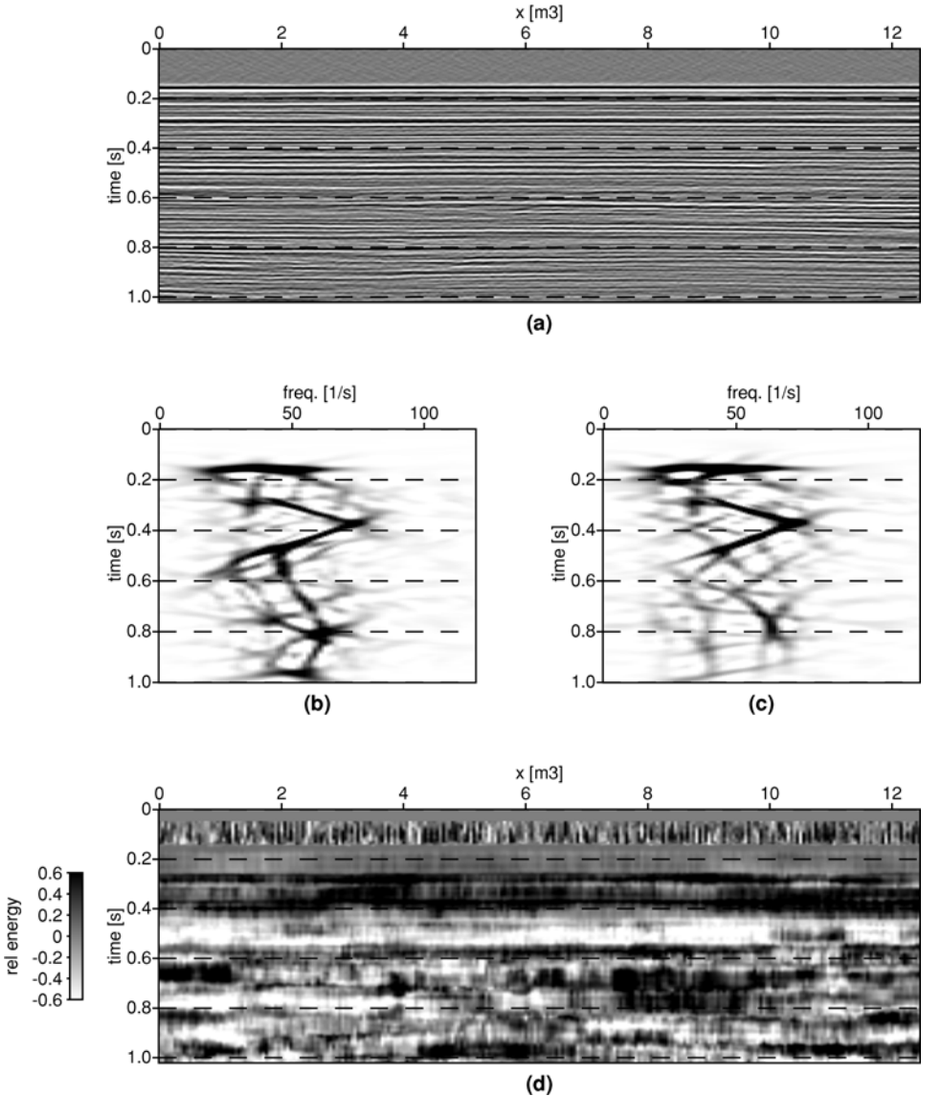

FIG. 5. (a) Seismic section, time-frequency representations of the (b) first and (c) last trace of the section, and (d) sequence classification.

$f^m(t)$ remain equivalent. For attribute extraction, we prefer kernels for which these constraints do not hold, since we want to replace the complex-trace instantaneous frequency by a more robust estimate of local average frequency. Using an optimum kernel time-frequency to compute the average frequency, some of the less desirable properties of the complex-trace instantaneous frequency, such as its tendency to go negative and its sensitivity to noise, can be avoided.

Figure 6 shows a seismic trace, its complex-trace instantaneous frequency obtained by phase differentiation, and the mean frequency obtained from an optimal kernel time-frequency representation. The complex-trace instantaneous frequency has anomalously high and low values that obscure more subtle variations of frequency content. The mean frequency as obtained from the optimum kernel time-frequency representation appears to be a more reliable indicator of the dominant frequency. Figure 7 shows a part of a migrated seismic section, the local average frequency of the data as extracted from an optimum kernel time-frequency representation, and the instantaneous frequency that was obtained by complex-trace analysis. For each trace in the section, the optimum kernel was computed using the method described in Baraniuk and Jones (1993b). We then estimated the average frequency of the resulting time-frequency representation using equation (9). Fine detail that is difficult to observe in the original section is brought out by the mean frequency display. The high frequency event at about 0.35 s can also be observed in the time-frequency representations of Figure 5. The event marks the lower boundary of the upper subunit that was observed in the seismic facies analysis of the same seismic section. In the mean frequency display, this boundary shows up as a highly correlative event, which is not easily recognized in the original section. Note also that reflection terminations can be much better identified in the mean frequency display than in the original section. Besides the instantaneous amplitude and instantaneous frequency, many other attributes can be defined within the time-frequency analysis framework. A logical step is to introduce the local higher-order moments in order to more accurately describe the characteristics of the local power spectrum.

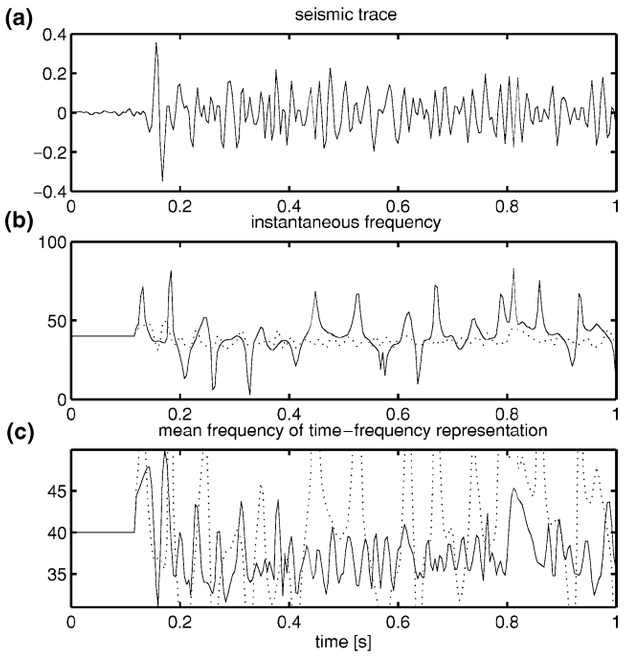

FIG. 6. (a) A seismic trace, (b) complex-trace instantaneous frequency obtained by phase differentiation, and (c) mean frequency of the adaptive optimal kernel time-frequency representation of the trace. For comparison, the dotted line in (b) is the solid line in (c), and the dotted line in (c) is the solid line in (b).

The instantaneous bandwidth, which was introduced by Barnes (1993b) as a complex-trace attribute, can also be estimated from the local spectrum. Local bandwidth $\sigma(t)$, defined as the variance around the mean frequency $f^m(t)$ is given by

$$\sigma(t)^2 = \frac{\int (f - f^m(t))^2 P(t; f)\, df}{E(t)}. \qquad (10)$$

Other measures that are used in statistics to characterize density functions are the skewness and kurtosis (Childers, 1997). Skewness is a measure for the deviation of the density function from a normal (Gaussian) distribution and is related to the third moment around the mean. A measure of the skewness of the local power spectrum is given by

$$s(t) = \frac{\int (f - f^m(t))^3 P(t; f)\, df}{\sigma(t)^3 E(t)}. \qquad (11)$$

A positive skewness signifies an asymmetric distribution with a tail extending out towards positive frequencies. A normal distribution has skewness zero. Kurtosis is used as a measure for the peakedness of the distribution. Using the usual definition, the kurtosis of a time-frequency representation as a function of time is given by

$$k(t) = \frac{\int (f - f^m(t))^4 P(t; f)\, df}{\sigma(t)^4 E(t)} - 3, \qquad (12)$$

where the term -3 makes the value zero for a normal distribution. Density functions with a positive kurtosis have a more sharply peaked shape than a Gaussian. Negative kurtosis signifies a distribution that is flatter than a normal distribution.

Figure 8 shows the higher order attributes for the seismic section of Figure 7. Skewness values range between -2 and 2 and kurtosis values range between -2 and 6. Interpretation of these attributes is not straightforward. Their usefulness for seismic interpretation should be assessed in terms of the significance that can be attached to the width, symmetry and peakedness of the local spectrum as a function of time. However, from the figure, some tentative conclusions can be drawn. The local bandwidth appears to be related to the uniformity of reflection spacing. Uniformly spaced events tend to show up as regions of relatively low bandwidth. In Figure 8a, this is most clearly observed for the events around 0.5 s traveltime. Below 0.5 s, there is relatively much bandwidth variation across traces, indicating a spatial change in reflection characteristics. High skewness value appear to indicate a facies transition. In a previous section, we proposed a subdivision of this seismic section into two facies units (Figure 5). The upper unit (0.16–0.5 s) was further divided into two subunits. The boundary between the two subunits is clearly visible at 0.35 s traveltime. We can also clearly observe the boundary between the upper and lower unit at 0.5 s. In the image of the kurtosis, we observe relatively high kurtosis values below 0.5 s. Below 0.5 s, the events are less

continuous and less regularly spaced that in the upper unit. The higher degree of disorder in the lower section is expressed in a more peaked character of the local spectrum. This relation is also known in other areas of seismic data analysis. In minimum entropy wavelet deconvolution, kurtosis is used as a heuristic measure for entropy (Wiggins, 1985). There are, of course, many other attributes that could be defined. Here, we have chosen to illustrate only those that appear relevant in the context of a statistical description. Other measures that may be defined are cumulative energies, peak counts, and spectral fall-off rates.

DISCUSSION

The relation between time-frequency representations and seismic attributes was first pointed out in the geophysical literature by Bodine (1986). In his paper, he argued that a local frequency measurement from this energy density is best obtained at a location where the energy is greatest. He proposed the measurement of frequency and phase at peaks of the trace envelopes, and named these attributes *response phase* and *response frequency* (White, 1991). From a time-frequency analysis perspective, it is immediately clear why these measures often perform better for waveform classification of seismic signal than the complex-trace attributes for all samples of the trace. Several theoretical explanations can be given, based on the relation between the rate of change of the envelope and the variance of instantaneous frequency (see, e.g., Robertson and Nogami, 1984; Cohen, 1995). A more intuitive explanation is given by the observation that strong cross terms in the time-frequency representation will be located between two envelope peaks. These cross terms do not contain information about the signal at that particular location but are generated by the interaction of the two neighboring peaks. In addition, for seismic signals, the instantaneous frequency generally has sharp peaks or negative values. These spikes may in some cases be used to indicate overlapping thin bed reflections, but they often also

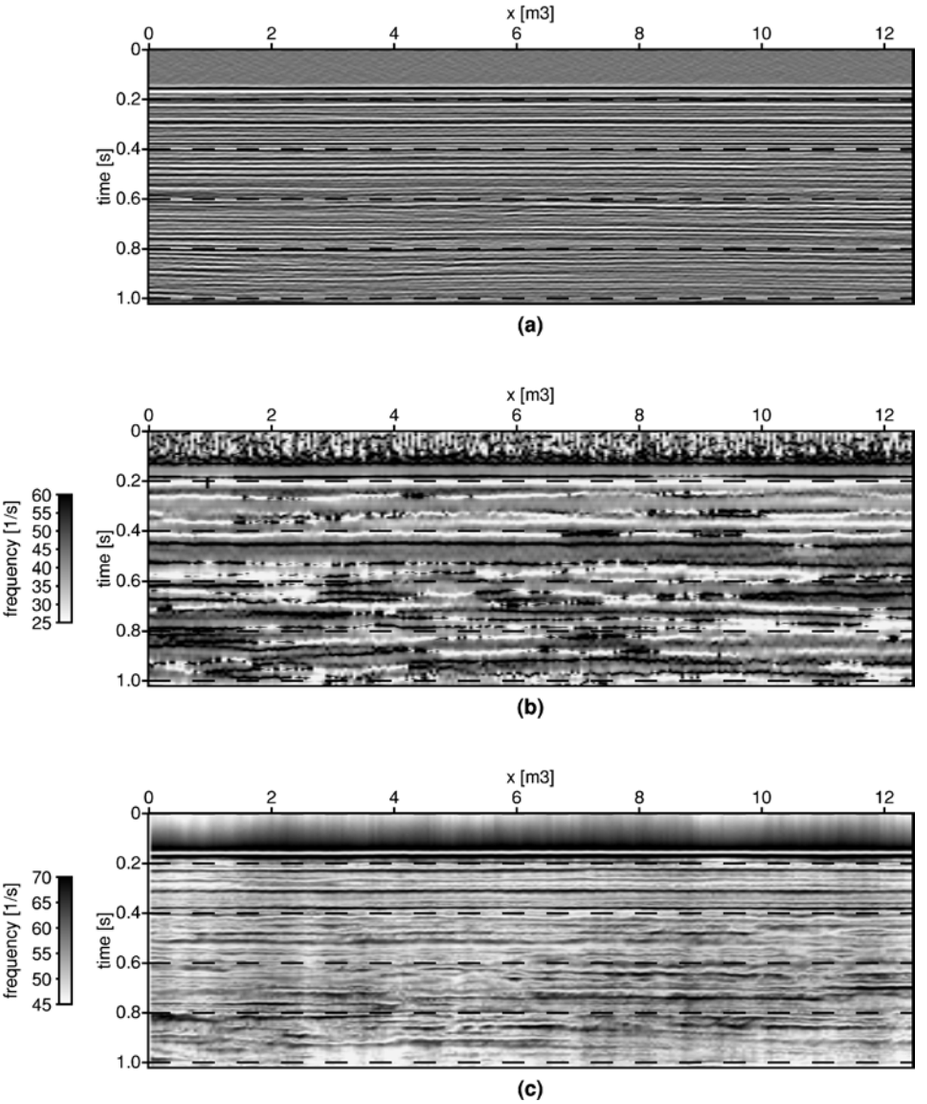

FIG. 7. (a) Seismic section, (b) complex-trace instantaneous frequency, (c) mean frequency of an optimal kernel time-frequency representation.

obscure much of the detailed information in the rest of the instantaneous frequency display. Furthermore, these negative values are outside the bandwidth of the signal, and the physical interpretation of instantaneous frequency as an average spectral frequency is lost (see, e.g., Barnes, 1993a). The occurence of sharp peaks and negative values in the instantaneous frequency can also be explained by an analysis of the cross terms. Since the cross terms attain negative values and will dominate the time-frequency representation between two strong components, the mean frequency at this location may also become negative. To mitigate this problem, we propose to use the optimally smoothed time-frequency representation for attribute extraction. The degree of cross-term suppression and time-frequency smoothing are inversely proportional. The adaptive kernel time-frequency approach provdes a flexible way of manipulating this trade-off between resolution and signal-to-noise ratio, depending on the application. For instance, robust attribute estimation can be achieved by choosing the degree of smoothing such that the average frequency remains within the bandwidth of the signal. This method has a significant advantage over the response attributes. The characteristics of the trace are extracted on a sample-by-sample basis, instead of only at envelope peaks. As a result, more detailed time information will be incorporated in the attribute analysis.

CONCLUSIONS

Time-frequency analysis is an effective method for studying the contribution of the subsurface reflectivity of to the spectral content of seismic data. A highly readable image of the local spectral content of the data can be obtained by using a time-frequency representation that is adapted to the signal under analysis. The time-frequency representation can aid in the classification of seismic sequences and serve as a validation tool for seismic facies interpretation. In addition, the theory of time-frequency representations provides a framework for

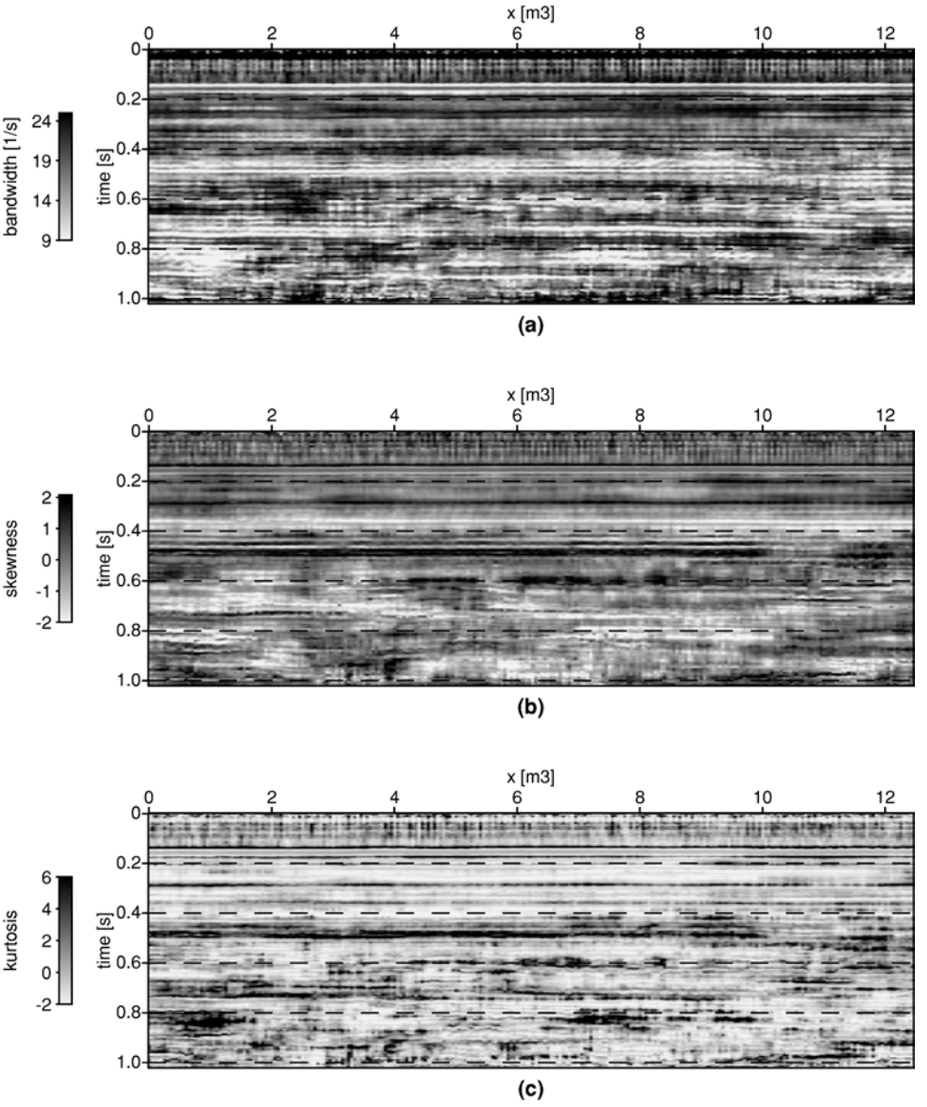

FIG. 8. (a) Instantaneous bandwidth, (b) instantaneous skewness, and (c) instantaneous kurtosis of the seismic section of Figure 10a.

complex-trace attribute extraction. In this framework, the attributes are parameters that describe the shape of a local spectrum, such as average frequency or bandwidth. Using the time-frequency representation, the signal-to-noise ratio of the attribute can be improved considerably without significant loss of time resolution. An additional advantage of attribute extraction from the time-frequency representation is the possibility of extending the basic set of complex-trace attributes with higher-order spectral measures, such as instantaneous bandwidth, skewness, and kurtosis.

ACKNOWLEDGMENTS

This research was carried out while the first author was at Delft University of Technology, The Netherlands, and was sponsored by TOMA, a cooperation between marine earth science groups in The Netherlands. We thank Prof. A. Maldonado of the University of Granada, Spain, for making the seismic data available to us. The support and contribution of Dr. John Woodside of the Free University of Amsterdam is gratefully acknowledged.

REFERENCES

Baraniuk, R. G., and Jones, D. L., 1993a, Signal dependent time-frequency analysis using a radially Gaussian kernel: Signal Processing, **32**, 263–284.
——— 1993b, A signal-dependent time-frequency representation: Optimal kernel design: IEEE Trans. Signal Processing, **41**, 1589–1602.
——— 1994, A signal-dependent time-frequency representation: Fast algorithm for Optimal kernel design: IEEE Trans. Signal Processing, **42**, 134–146.
Barnes, A. E., 1993a, When the concepts of spectral frequency and instantaneous frequency converge: The Leading Edge, **12**, 1020–1023.
——— 1993b, Instantaneous spectral bandwidth and dominant frequency with applications to seismic reflection data: Geophysics, **58**, 419–428.
Bodine, J. H., 1986, Waveform analysis with seismic attributes: Oil & Gas J., **84**, No. 23, 59–63.
Claasen, T. A. C. M., and Mecklenbräuker, W. F. G., 1980, The Wigner distribution—A tool for time-frequency signal analysis—Part I: Continuous time signals: Philips J. Res., **35**, 217–250.
Childers, D. G., 1997, Probability and random processes: Irwin.
Cohen, L. 1989 Time-frequency distributions—A review: Proc. IEEE, **77**, 941–981.
——— 1995, Time-frequency analysis: Prentice-Hall, Inc.
Fokkema, J. T., and Ziolkowski, A. M., 1987, The critical reflection theorem: Geophysics, **52**, 965–972.
Fuchs, K., and Müller, G., 1971, Computation of synthetic seismograms with the reflectivity method and comparison with observations: Geophys. J. Roy. Astr. Soc., **23**, 417–433.
Hlawatsch, F., and Boudreaux-Bartels, G. F., 1992, Linear and quadratic time-frequency signal representations: IEEE Signal Processing Magazine, **9**, No. 2, 21–67.
Jones, D. L., and Baraniuk, R. G., 1995, An adaptive optimal-kernel time-frequency representation: IEEE Trans. Signal Processing, **43**, 2361–2371.
Jurado, M. J., and Comas, M. C., 1992, Well log interpretation and seismic character of the Cenozoic sequence in the northern Alboran Sea: Geo-Marine Letters, **12**, 129–136.
Morlet, J., Arens, G., Fourgeau, E., and Giard, D., 1982, Wave propagation and sampling theory—Part I: Complex signal and scattering in multilayered media: Geophysics, **47**, 203–221.
Robertson, J. D., and Nogami, H. H., 1984, Complex seismic trace analysis of thin beds: Geophysics, **49**, 344–352.
Steeghs, T. P. H., 1997, Local power spectra and seismic interpretation: Ph.D. diss., Delft Univ. of Technology.
Taner, T. H., Koehler, F., and Sheriff, R. E., 1979, Complex seismic trace analysis: Geophysics, **44**, 1041–1063.
Taner, T. H., and Sheriff, R. E., 1977, Applications of amplitude, frequency and other attributes to stratigraphic and hydrocarbon determination, *in* Payton, C. E. Ed., Seismic stratigraphy—Applications to hydrocarbon exploration: Am. Assn. Petr. Geol. Memoir **26**, 301–328.
White, R. E., 1991, Properties of instantaneous seismic attributes: The Leading Edge, **10**, No. 7, 26–32.
Wiggins, J. W., 1985, Entropy-guided deconvolution: Geophysics, **40**, 2720–2726.

APPENDIX A

QUADRATIC TIME-FREQUENCY REPRESENTATIONS

In this appendix, we discuss the relation between the attributes that are obtained from the analytic signal and the time-frequency representations of the quadratic class.

In the context of signal analysis, an analytic signal is a complex-valued signal with real and imaginary parts that are their respective Hilbert transforms. The complex-trace attributes as used in seismic interpretation are closely related to the notion of the analytic signal (Taner et al., 1979). The imaginary part of the analytic seismic signal is found by a Hilbert transformation of the real signal $s(t)$:

$$\mathrm{Im}\{u^a\}(t) = \mathcal{H}\{s\}(t), \tag{A-1}$$

where $\mathcal{H}\{s\}$ denotes the Hilbert transformation of u with respect to time. For the analytic signal, the following nomenclature is widely used. Given the signal

$$u^a(t) = s(t) + \mathrm{j}\mathcal{H}\{s\}(t) = a(t)\exp(\mathrm{j}2\pi\phi(t)), \tag{A-2}$$

the following terms are used:

$a(t) = \sqrt{s(t)^2 + \mathcal{H}\{s\}(t)^2}$ is the *modulus* or *envelope*,

$\phi(t) = \tan^{-1}\left\{\dfrac{\mathcal{H}\{s\}(t)}{s(t)}\right\}$ is the *argument* or *phase*.

Because the envelope and phase of the analytic signal are functions of time—as opposed to the spectral amplitude and phase functions—they are often called *instantaneous* amplitude and *instantaneous* phase. An important parameter is the derivative of the phase with time,

$$f^c(t) = \frac{1}{2\pi}\frac{d\phi(t)}{dt}, \tag{A-3}$$

where $f^c(t)$ is the *instantaneous frequency*. In seismic signal analysis, the instantaneous amplitude, instantaneous phase and instantaneous frequency are called the *complex-trace attributes*.

Complex-trace attributes and the Wigner distribution

The complex-trace attributes can also be derived as parameters that describe the Wigner distribution of a signal. The Wigner distribution is a local power spectrum that is obtained by a Fourier transformation of a local autocorrelation function. The instantaneous autocorrelation function of a signal $u(t)$ is defined as

$$R(t;\tau) = u\left(t + \frac{1}{2}\tau\right)u^*\left(t - \frac{1}{2}\tau\right). \tag{A-4}$$

The Wigner distribution $W(t; f)$ of a signal $u(t)$ is then given by

$$W(t; f) = \int_{\tau\in\mathbb{R}} \exp(-\mathrm{j}2\pi f\tau) u\left(t + \frac{1}{2}\tau\right) u^*\left(t - \frac{1}{2}\tau\right) d\tau = \mathcal{F}_\tau^-\{R(t; \tau)\}, \quad \text{(A-5)}$$

where the asterisk denotes complex conjugation. In this appendix, we use the notation $\mathcal{F}_a^-\{u\}$ to denote a Fourier transformation of u over variable a, where the superscript denotes the sign in the exponent. The Wigner distribution has many attractive mathematical properties (Cohen, 1995; Steeghs, 1997). Some of these properties are of particular interest in the context of seismic attribute analysis. Integration of the Wigner distribution over time yields the spectral energy density spectrum $E(f)$ of the signal, i.e.,

$$E(f) = \int_{t\in\mathbb{R}} W(t; f)\, dt = |\hat{u}(f)|^2. \quad \text{(A-6)}$$

In the same fashion, integration of the Wigner distribution over frequency yields the instantaneous energy $E(t)$ of the signal, i.e.,

$$E(t) = \int_{f\in\mathbb{R}} W(t; f)\, df = |u(t)|^2. \quad \text{(A-7)}$$

For an analytic signal, $E(t)$ is the *instantaneous power* of reflection strength, which is the square of the instantaneous amplitude or envelope of the signal. $E(f)$ and $E(t)$ are called, respectively, the *frequency marginal* and *time marginal* of the distribution.

The instantaneous frequency of the complex trace is equal to the mean frequency as a function of time of the Wigner distribution. The relative first-order moment of the Wigner distribution with respect to frequency is given by

$$\langle f\rangle_t = \frac{1}{E(t)} \int_{f\in\mathbb{R}} f\, W(t; f)\, df, \quad \text{(A-8)}$$

where the brackets denote the average and the underscore t that this average is taken for every time t. The average frequency of the Wigner distribution can also be obtained directly from the signal. Equation (A-8) can also be written as an inverse Fourier transformation:

$$\langle f\rangle_t = \frac{1}{E(t)} \mathcal{F}_f^+\{f W(t; f)\}(t; \tau = 0). \quad \text{(A-9)}$$

With the definition of $W(t; f)$ of equation (A-5), we obtain

$$f W(t; f) = \frac{1}{\mathrm{j}2\pi} \mathcal{F}_\tau^-\{\partial_\tau R(t; \tau)\}. \quad \text{(A-10)}$$

Substitution of equation (A-10) in the right-hand side of equation (A-9) leads to

$$\langle f\rangle_t = \frac{1}{\mathrm{j}2\pi E(t)} \partial_\tau R(t; \tau)|_{\tau=0}. \quad \text{(A-11)}$$

We now substitute the definition of $R(t; \tau)$ of equation (A-4) and perform the differentiation. We then obtain an expression of the average frequency in terms of the signal $u(t)$, given by

$$\langle f\rangle_t = \frac{\mathrm{j}}{4\pi E(t)} \left[u(t)\partial_t u^*(t) - u^*(t)\partial_t u(t)\right]. \quad \text{(A-12)}$$

Using $E(t) = u(t)u^*(t)$, we can further simplify this result and arrive at

$$\langle f\rangle_t = \frac{1}{2\pi} \mathrm{Im}\left\{\frac{\partial_t u(t)}{u(t)}\right\} = \frac{1}{2\pi} \mathrm{Im}\{\partial_t \ln u(t)\}. \quad \text{(A-13)}$$

In the case that $u(t)$ is an analytic signal [equation (A-2)], we have

$$\langle f\rangle_t = \frac{1}{2\pi} \mathrm{Im}\{\partial_t \ln[a(t)\exp(\mathrm{j}\phi(t))]\} = \frac{1}{2\pi} \partial_t \phi(t) = f^c(t), \quad \text{(A-14)}$$

where $\phi(t)$ is the *instantaneous phase* and $f^c(t)$ is the *instantaneous frequency* of the analytic signal. Hence, we can obtain the complex-trace instantaneous frequency of a signal as the average frequency as a function of time of the Wigner distribution of the signal.

General class of quadratic time-frequency representations

In the two-dimensional Fourier transform of the Wigner distribution, smoothing of the Wigner distribution can be conveniently replaced by a simple weighting operation. In order to reduce the interference by cross terms in the Wigner distribution, the application of a low-pass window to the ambiguity function may be an effective approach because the cross terms occupy the region away from the origin in this domain.

A time-frequency representation $P(t; f)$ is related to its characteristic function $M(\nu; \tau)$ by a Fourier transformation with respect to the correlation variables ν and τ. The characteristic function of the Wigner distribution is the ambiguity function, given by

$$A(\nu; \tau) = \int_{t\in\mathbb{R}} \int_{f\in\mathbb{R}} \exp(-\mathrm{j}2\pi(\nu t - f\tau)) W(t, f)\, dt\, df. \quad \text{(A-15)}$$

The ambiguity function can also be expressed in terms of the local autocorrelation function equation (A-4) as

$$A(\nu; \tau) = \mathcal{F}_t^-\{R(t; \tau)\}. \quad \text{(A-16)}$$

The application of a filter on the ambiguity function results in the new time-frequency representation, given by

$$P(t; f) = \mathcal{F}_\nu^+ \mathcal{F}_\tau^-\{M(\nu; \tau)\}, \quad \text{(A-17)}$$

where the characteristic function $M(\nu; \tau)$ is the weighted ambiguity function, i.e.,

$$M(\nu; \tau) = \Psi(\nu; \tau) A(\nu; \tau). \quad \text{(A-18)}$$

Integration of the Wigner distribution over frequency yields the instantaneous energy [cf. equation (A-7)]. This property is referred to as the time marginal property. If we want to retain this property in a representation from the general class, we require that

$$\int_{f\in\mathbb{R}} P(t; f)\, df = |u(t)|^2. \quad \text{(A-19)}$$

This requirement is fulfilled if

$$\Psi(\nu; 0) = 1, \quad \text{for } \nu \in \mathbb{R}. \quad \text{(A-20)}$$

Requiring the frequency marginal property

$$\int_{t\in\mathbb{R}} P(t;\, f)\, dt = |u(f)|^2 \tag{A-21}$$

leads to the condition

$$\Psi(0, \tau) = 1, \quad \text{for } \tau \in \mathbb{R}. \tag{A-22}$$

We showed in the previous section that the average frequency as a function of time of the Wigner distribution is the derivative of the temporal phase of the analytic signal. The mean frequency as a function of time $f^m(t)$ of the time-frequency representation $P(t;\, f)$ is given by

$$f^m(t) = \frac{\displaystyle\int_{f\in\mathbb{R}} f\, P(t;\, f)\, df}{\displaystyle\int_{f\in\mathbb{R}} P(t;\, f)\, df}. \tag{A-23}$$

If we want to retain the local average frequency of the Wigner distribution in the smoothed Wigner distribution, we must require that

$$\lim_{\tau\to 0} \Psi(\nu;\, \tau) = 1, \text{ for } \nu \in \mathbb{R}, \tag{A-24}$$

which is the constraint for the frequency marginal property, and also

$$\lim_{\tau\to 0} \partial_\tau \Psi(\nu;\, \tau) = 0, \text{ for } \nu \in \mathbb{R}. \tag{A-25}$$

Optimum kernel design for cross-term suppression

Figure A-1 shows the Wigner distribution and ambiguity function of a seismic signal (see also Figure 1). The cross-terms distribution is strongly oscillating ridges that are the result of the quadratic nature of the Wigner distribution. The Wigner distribution of the sum of two signals $u_1(t)$ and $u_2(t)$ is given by (Hlawatsch and Boudreaux-Bartels, 1992)

$$W_{u_1+u_2}(t;\, f) = W_{u_1}(t;\, f) + W_{u_2}(t;\, f) + 2\mathrm{Re}\{W_{u_1u_2}(t;\, f)\}, \tag{A-26}$$

where $W_{u_1u_2}(t;\, f)$ is the *cross-Wigner distribution* of the two signals u_1 and u_2, defined as

$$W_{u_1u_2}(t;\, f) = \int \exp(-\mathrm{j}2\pi f\tau) u_1\left(t + \frac{1}{2}\tau\right) u_2^*\left(t - \frac{1}{2}\tau\right) d\tau. \tag{A-27}$$

W_{u_1} and W_{u_2} are referred to as auto terms, and $W_{u_1u_2}$ is the cross term. In the Fourier transform of the Wigner distribution (the ambiguity function), the highly osccillating cross terms are generally mapped to locations away from the origin, whereas

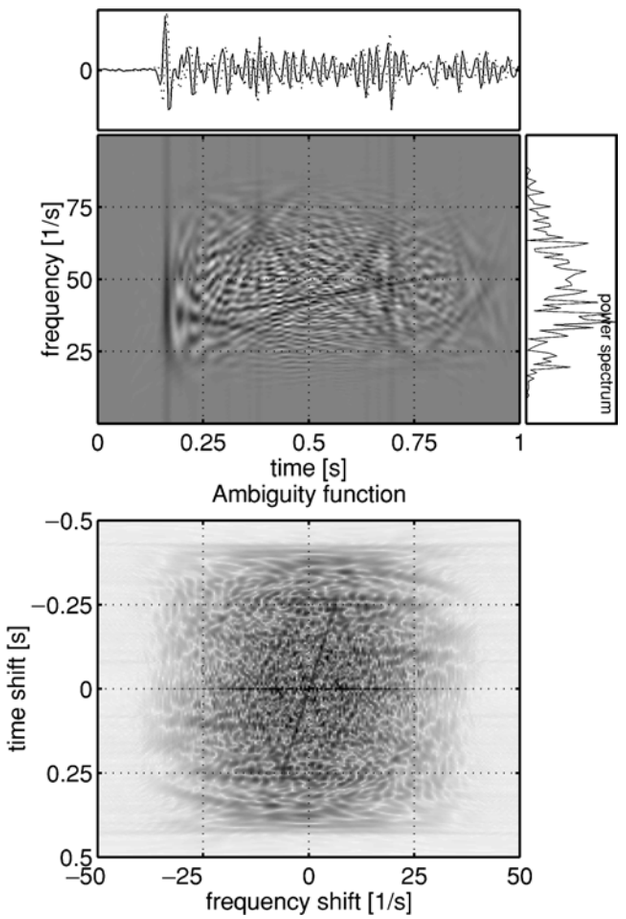

FIG. A-1. Wigner distribution and ambiguity function of a seismic trace.

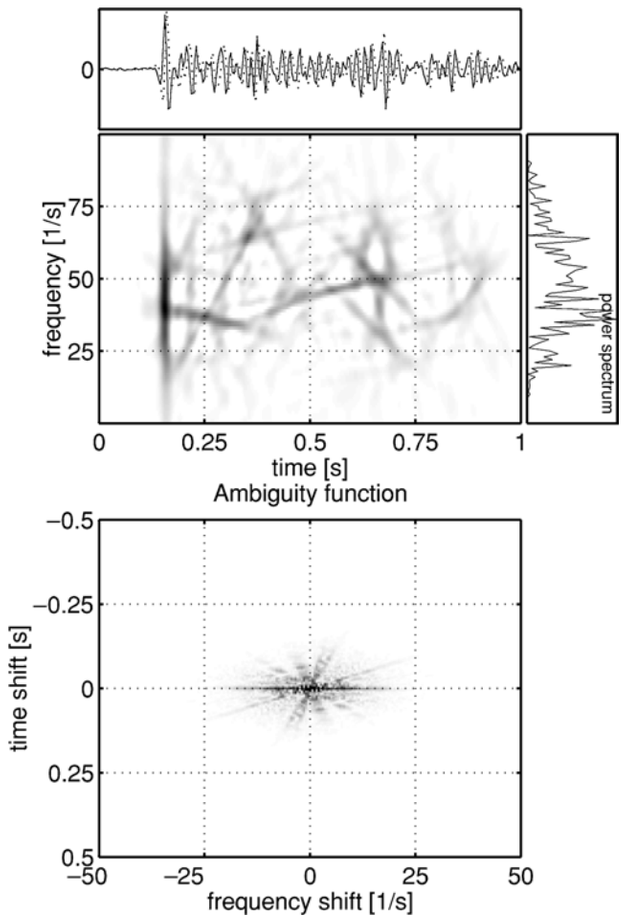

FIG. A-2. Adaptive optimum kernel time-frequency representation and ambiguity function of a seismic trace.

the auto terms are located near the origin. In order to suppress the cross terms, the application of a low-pass two-dimensional filter on the ambiguity function of the signal is usually very effective. However, the size and shape of the region that is occupied by the auto terms is different for each signal. Consequently, a filter that with a fixed shape can only achieve satisfactory cross-term suppresion for a limited class of signals. The poor performance of fixed filters for signals with properties that vary strongly over time has lead to the design of algorithms for signal-adaptive optimum kernels for cross-term suppression (Baraniuk and Jones, 1993a, 1993b; Jones and Baraniuk, 1995). The optimum smoothing function is found by adapting the filter to the shape of the auto terms of the signal in the ambiguity function. First, the degree of smoothing is specified by a parameter that fixes the size of the pass region of the low-pass filter. The shape of the filter is then adapted to maximize the energy in the pass band. Figure A-2 shows the time-frequency representation and ambiguity function that is obtained by adapting a radially Gaussian filter to the signal (Baraniuk and Jones, 1993a). The cross terms have been largely suppressed, while at the same time distortion of the auto terms has been minimized by adapting the filter shape to the characteristics of the signal. A further refinement of the method is to adapt the shape of the kernel as a function of time (Jones and Baraniuk, 1995). Most of the time-frequency representations of seismic data we show in this paper were generated with this method. However, for attribute extraction, this method is less suitable because of the computational effort that is required for adapting the kernel for each time sample. The examples of Figures 7 and 8 were generated using the optimal kernel method that is described in in Baraniuk and Jones (1993b, 1994). The number of operations to compute the global optimum kernel time-frequency representation is typically in the order of the $N^2 \log N$ for a trace of length N.